

Original Research

Study on $\text{Cr}_2\text{O}_3/\gamma\text{-Al}_2\text{O}_3$ Catalysts for Mixed Pyrolysis of Coal to Produce Hydrogen-Rich Fuel Gas

Chen Jihao^{1,3*}, Li Yue¹, Zhang Lei²

¹Shaanxi Coal Geological Laboratory Co.,Ltd., Xi'an, 710054, China

²Xi'an University of Science and Technology, Xi'an, 710054, China

³Key Laboratory of Coal Resources Exploration and Comprehensive Utilization, Ministry of Natural Resources, Xi'an, 710021, China

Received: 4 March 2021

Accepted: 13 April 2021

Abstract

$\gamma\text{-Al}_2\text{O}_3$ was used as the carrier, the group VIII metal oxides and the sub group metal oxides were used as active components, and the $\gamma\text{-Al}_2\text{O}_3$ catalysts were prepared by the equal volume impregnation method. Hydrogen rich fuel gas and tar products were produced by the mixed pyrolysis of coal and catalysts in a furnace. The influence of $\gamma\text{-Al}_2\text{O}_3$ catalysts with different loading Cr_2O_3 on the mixed pyrolysis products of coal was studied. The catalyst was characterized by ICP-MS, XRD and BET, and the pyrolysis mechanism of coal and catalyst was studied. The results showed that: 1) The tar and gas of coal pyrolysis were 0.32g and 1.58g, respectively, and the highest total contents of CO, H₂ and CH₄ were 71.40% respectively. 2) $\text{Fe}_2\text{O}_3/\gamma\text{-Al}_2\text{O}_3$ catalyst made the highest tar of 0.75g, which was 16.4% higher than that of coal; $\text{Cr}_2\text{O}_3/\gamma\text{-Al}_2\text{O}_3$ catalyst made the highest gas of 1.73g, which was 9.5% higher than that of raw coal. 3) The $\text{Cr}_2\text{O}_3/\gamma\text{-Al}_2\text{O}_3$ catalyst prepared by loading 1% Cr_2O_3 had better catalytic effect. 4) The specific surface areas of $\text{Cr}_2\text{O}_3/\gamma\text{-Al}_2\text{O}_3$ and $\gamma\text{-Al}_2\text{O}_3$ were similar, while the catalytic cracking effect of $\text{Cr}_2\text{O}_3/\gamma\text{-Al}_2\text{O}_3$ was more obvious than that of $\gamma\text{-Al}_2\text{O}_3$, so Cr_2O_3 improved the catalytic activity.

Keywords: group VIII metal oxides, sub-group metal oxides, mixed pyrolysis, hydrogen rich fuel gas, tar

Introduction

Coal is a valuable energy resource, but also a complex compound, containing many kinds of chemical substances, and a variety of chemical raw materials can be refined through pyrolysis coal. In the process of coal pyrolysis, tar, pyrolytic gas and pyrolytic

coke are mainly produced [1]. At the same time, the utilization efficiency and comprehensive utilization value of coal can be improved by pyrolysis, and the environmental pollution caused by direct combustion can also be reduced [2]. The main components of coal pyrolysis gas are O₂, N₂, H₂, CO, CO₂, CH₄, CnH_m and so on. The combustible gases which can be used in pyrolysis gas are H₂, CO, CH₄ and so on. They can be used as industrial fuel for power generation and city gas. The pyrolysis gas products and yields

*e-mail: 15929995059@163.com

of coal are quite different due to the different types and pyrolysis conditions of coal. The composition and distribution of pyrolysis products vary with the degree of coalification, the structure and properties of coal, and the H/C, O/C, fixed carbon and volatile matter in coal. The activation energy increased with the increase of the degree of coalification and the temperature at the beginning of pyrolysis [3]. The pyrolysis temperature is the main external factor that affects the coal pyrolysis. When the pyrolysis temperature rises, the pyrolysis gas yield increases, but the solid coke and pyrolysis tar yield decreases correspondingly. The effect of pyrolysis temperature on the pyrolysis gas of lignite at low temperature [4]. The results showed that with the increase of pyrolysis temperature, the yields of CO and CO₂ increased first and then decreased, while the yields of CH₄ and H₂ increased gradually. At higher temperature, the prolongation of the residence time will increase the degree of the secondary reaction and influence the distribution of pyrolytic products [5]. The pressure in the pyrolysis system of coal will affect the mass transfer process in the pyrolysis process, and the increase of the pressure will increase the resistance of the release of the primary volatiles, prolong the residence time, and lead to the intensification of the secondary reaction of the volatiles [6]. The yield of catalyst gas is the most important factor, which can increase the content of combustible gas in pyrolysis gas and improve the quality of coal tar to some extent [7]. The results showed that the main components of pyrolysis gas were H₂, CO, CO₂, CH₄ and CnHm, and each component of pyrolysis gas was produced by pyrolysis and polycondensation of specific functional groups in coal. Among them, CO and CO₂ were related to the oxygen-containing functional groups in coal; hydrocarbon gas was related to the side chain of fat; it was mainly related to the condensation reaction. At low temperature, CO₂ mainly produced in the cracking of carboxyl, carbonyl and ester groups, while CO mainly produced in the cracking of carbonyl groups; at high temperature, CO₂ mainly produced in the relatively stable oxygen-containing functional groups (ether, quinone, oxygen-containing heterocycle, etc.) and carbonate minerals, while CO mainly produced in the cracking of quinone, ester ether, aromatic ether and phenol hydroxyl [8]. At low temperature, CH₄ produced by the breaking of methoxy group in aromatic side chain; when the temperature risen to 500-550°C, CH₄ produced by the breaking of methylene bridge bond and methyl; at high temperature, CH₄ produced by the breaking of aromatic heterocycle and hydrogen carbon reaction [9]. The amount of pyrolysis gas released during coal pyrolysis was very small, and CnHm mainly came from aromatic aliphatic side chain fracture, cracking and condensation of aliphatic hydrocarbons [10]. Compared with other pyrolysis gas components, H₂ was generated at a higher temperature, and it generated at about 400°C. Most researchers believed that H₂ mainly came

from coal dehydrogenation (condensation of organic matter, cyclization and aromatization of alkanes) and reaction with water [11], and some scholars believed that it also came from the reaction of water gas at high temperature [12].

At present, there was many kinds of catalysts for coal catalytic pyrolysis, many of which have excellent performance and can be used in industrial production are composed of catalyst carrier and active components. The support of the catalyst can ensure that the catalyst is suitable for different catalytic environments, and the active component can ensure the catalytic efficiency of the catalyst. γ -Al₂O₃ has excellent physical and chemical properties [13], and can maintain high mechanical properties in different catalytic environments. As a carrier for preparing catalyst, it is very suitable for experimental operation and industrial application. There are many kinds of active components in catalysts. The selection of metal oxides is mainly in alkali metal oxides [14], alkaline earth metal oxides [15], by-group metal oxides [16] and the eighth group metal oxides [17]. Metal oxides are widely used as active components of catalysts, and have directional control effect on coal pyrolysis products. Therefore, the preparation of excellent catalyst is very important for the production and quality of combustible gas from coal pyrolysis.

In this study, γ -Al₂O₃ was used as the carrier to prepare the catalyst, and group VIII and sub-group metal oxides were used as the active components to support γ -Al₂O₃ to prepare the supported catalyst. The effect of the catalyst on the oil and gas production in the process of coal pyrolysis catalytic cracking was studied, and a kind of industrial application supported γ -Al₂O₃ catalyst with high catalytic efficiency was prepared, so as to improve the efficiency of coal pyrolysis production and the quality of hydrogen rich fuel gas.

Material and Methods

Materials and Drugs

The coal used in the experiment was produced in Cuimu Coal Mine, Shaanxi, with a particle size of 3~5 mm. Table 1 shows the results of industrial analysis and elemental analysis of the coal sample. γ -Al₂O₃ was purchased on the market with a particle size of 3~5mm. Fe(NO₃)₃·9H₂O, Co(NO₃)₂·6H₂O, Ni(NO₃)₂·6H₂O, Cu(NO₃)₂·3H₂O, (CH₂COO)₂Zn·2H₂O, (NH₄)₆Mo₇O₂₄·4H₂O, Cr(NO₃)₃·9H₂O and Mn(NO₃)₂·4H₂O were all analytically pure.

Preparation of Catalysts

(1) Preparation of γ -Al₂O₃ supported subgroup metal oxide catalyst: By constant volume impregnation, 3 g γ -Al₂O₃ was immersed in 5% Fe(NO₃)₃ solution for 24 h. It was taken out and placed in a muffle

Table 1. Industrial analysis and elemental analysis of coal samples (%).

Industrial analysis				Elemental analysis				
Mad	Aad	Vad	FCad	C	H	O	N	S
4.99	11.87	32.79	50.35	67.64	3.63	27.53	0.67	0.53

furnace and roasted at 450°C for 4h. It was removed as $Fe_2O_3/\gamma-Al_2O_3$ catalyst with 5% loading. $Co_2O_3/\gamma-Al_2O_3$ and $Ni_2O_3/\gamma-Al_2O_3$ catalysts with 5% loading were prepared by the same method.

(2) Preparation of $\gamma-Al_2O_3$ supported group VIII metal oxide catalyst: By constant volume impregnation, 3 g $\gamma-Al_2O_3$ was immersed in 5% $Cu(NO_3)_2$ solution for 24 h. It was taken out and placed in a muffle furnace and roasted at 450°C for 4h. It was removed as $CuO/\gamma-Al_2O_3$ catalyst with 5% loading. $ZnO/\gamma-Al_2O_3$, $Mo_2O_3/\gamma-Al_2O_3$, $Cr_2O_3/\gamma-Al_2O_3$ and $Mn_2O_3/\gamma-Al_2O_3$ catalysts with 5% loading were prepared by the same method.

(3) Preparation of $Cr_2O_3/\gamma-Al_2O_3$ catalysts with different loading loads: By constant volume impregnation, 3 g $\gamma-Al_2O_3$ was immersed in 1%, 5% and 11% $Cr(NO_3)_3$ solution for 24 h. It was taken out and placed in a muffle furnace and roasted at 450°C for 4 h. It was removed as $Cr_2O_3/\gamma-Al_2O_3$ catalyst with 1%, 5% and 11% loading.

Activity Evaluation of Catalyst

In the experiment, in the coal pyrolysis cracking catalytic system, 15 g coal sample and 3 g catalyst were mixed and placed at furnace was vacant. First, the coal undergoes a catalytic pyrolysis reaction, and the resulting pyrolysis product entered the tar collector. The liquid phase components of the catalytic pyrolysis were collected, and the gas phase components were dried. The gas was collected and detected by the gas collector. The dried gas entered the flowmeter to count the volume, and then it was collected and detected. At the end of the experiment, the tar attached in the reaction tube and condensation tube was washed with acetone, and all acetone solutions containing tar were collected together. The water in tar was collected by anhydrous sodium sulfate, and then the acetone was removed by rotary evaporation, and the tar was collected

and weighed. The gas components were detected by gas chromatography, and the changes of gas and tar components were analyzed. In this paper, the effect of catalyst was evaluated by the change of pyrolysis products of bituminous coal.

Detection of Pyrolysis Products

The gas produced by catalytic cracking of tar was collected by gas collecting bag and analyzed by GC-2014c gas chromatography. The working conditions of gas chromatography were shown in Table 2 below.

Characterization

The Vario EL III element analyzer (Elementar company in Germany) was used for elemental detection of coal samples.

Specific surface area (BET): The JW-BK122W type surface and pore size analyzer is used to measure the specific surface area of different types of the catalysts.

X-ray analysis (XRD, Beijing General Analysis Instrument Co., Ltd.): XD-3 type ray diffractometer; the test parameters: the voltage is 36 KV, the current is 20 mA, the target is Cu, K alpha rays, 2θ is 5° to 80°, and scanning speed is 4(°)/min.

Inductively coupled plasma mass spectrometer (ICP-MS): iCAP Q type, (Thermo Fisher Scientific, USA), working conditions, RF generator power: 1400 kw, cooling gas flow rate: 13.0 L/min, auxiliary gas flow rate: 0.72 L/min, scanning mode: peak jump, atomizer flow rate: 0.90 L/min, sampling time: 20s, sampling pump speed: 70 rpm, sampling depth: 150 mm, sampling cone: 1.1 mm, intercepting cone: 0.9 mm, double charge production Rate: $IBa^{++}/Ba < 3\%$, oxide yield, $ICeO^{+}/Ce < 3\%$, mainly used to determine the content of catalysts.

Table 2. Operating conditions of GC.

Detector	TCD	FID
Chromatographic column	Stainless steel column (3 m)	Stainless steel column (3 m)
Gasification chamber temperature (°C)	360	360
Column box temperature (°C)	80	80
Detector temperature (°C)	100	150
Determination of gases		

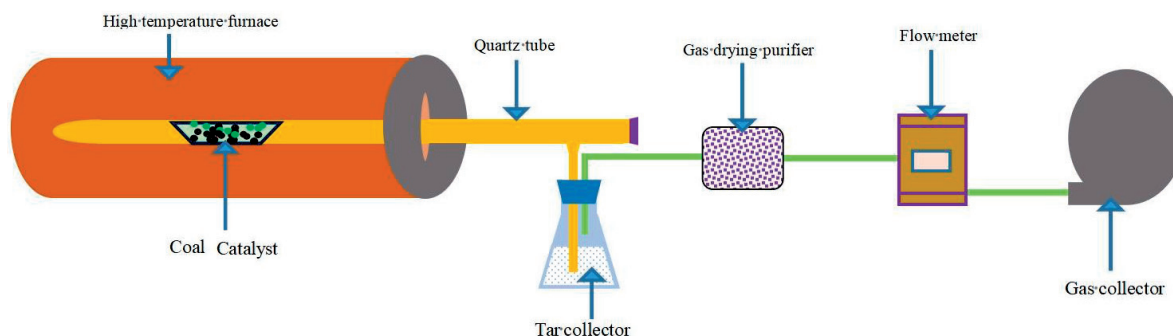


Fig. 1. Reaction device diagram.

Results and Discussion

Effect of Subgroup Metal Oxide Supported γ - Al_2O_3 Catalyst on Coal Pyrolysis Products

Effect of Subgroup Metal Oxide Supported γ - Al_2O_3 Catalyst on Gas and Tar

Fig. 2 showed the changes of gas products and tar under the conditions of final pyrolysis temperature 600°C and constant temperature of 5 min after mixing 15 g coal and g subgroup metal oxide supported γ - Al_2O_3 catalyst into pyrolysis furnace. As can be seen from Fig. 2, the tar yield and gas yield of raw coal pyrolysis were 0.75 g and 1.58 g respectively; and the tar and gas contents were improved by adding γ - Al_2O_3 , $\text{Fe}_2\text{O}_3/\gamma$ - Al_2O_3 , CoO/γ - Al_2O_3 and NiO/γ - Al_2O_3 in the process of coal pyrolysis $\text{Fe}_2\text{O}_3/\gamma$ - Al_2O_3 resulted in the highest tar yield of 0.75 g, which was 134.38% higher than that of raw coal; while CoO/γ - Al_2O_3 resulted in the highest gas yield of 1.65 g, which was 4.4% higher than that of raw coal. When coal and γ - Al_2O_3 were pyrolyzed together, the contact between coal and γ - Al_2O_3 resulted in the breaking of macromolecular chains in coal, which promoted the pyrolysis of coal and produced more pyrolytic products. The pyrolysis products entered

into γ - Al_2O_3 and came into contact with the active sites, which further lead to the breaking of macromolecules and the vaporization and volatilization of small molecules at higher temperatures, thus increasing tar yield. When γ - Al_2O_3 was loaded with Fe_2O_3 , Co_2O_3 and Ni_2O_3 , the active sites were increased on the surface and in the interior of γ - Al_2O_3 , which promoted the cracking of macromolecular substances and further increased the yield of tar and gas. Fe_2O_3 , Co_2O_3 and Ni_2O_3 were used as the active components, of which Fe_2O_3 was the most active.

Effect of Subgroup Metal Oxide Supported γ - Al_2O_3 Catalyst on Gas Components

Fig. 3 showed the mixture of 15 g coal sample and 3 g catalyst and pyrolysis in the pyrolysis furnace. Figs 3(a-e) respectively represented the raw coal, adding γ - Al_2O_3 catalyst, $\text{Fe}_2\text{O}_3/\gamma$ - Al_2O_3 catalyst, $\text{Co}_2\text{O}_3/\gamma$ - Al_2O_3 catalyst and NiO/γ - Al_2O_3 catalyst, and the gas composition changed with the pyrolysis temperature. As can be seen from Fig. 3, the variation trend of gas with pyrolysis temperature was basically the same after the addition of different catalysts. CH_4 content reach the maximum when the pyrolysis temperature reaches 500°C to 550°C . When the pyrolysis temperature reach

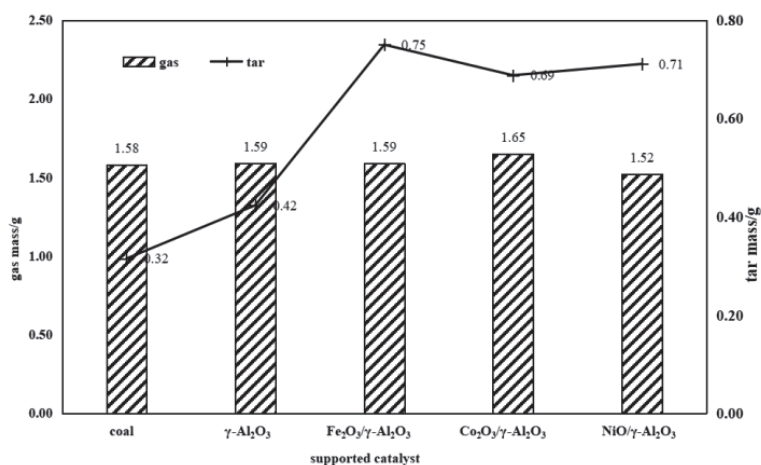


Fig. 2. Effect of subgroup metal oxide supported γ - Al_2O_3 catalyst on gas and tar.

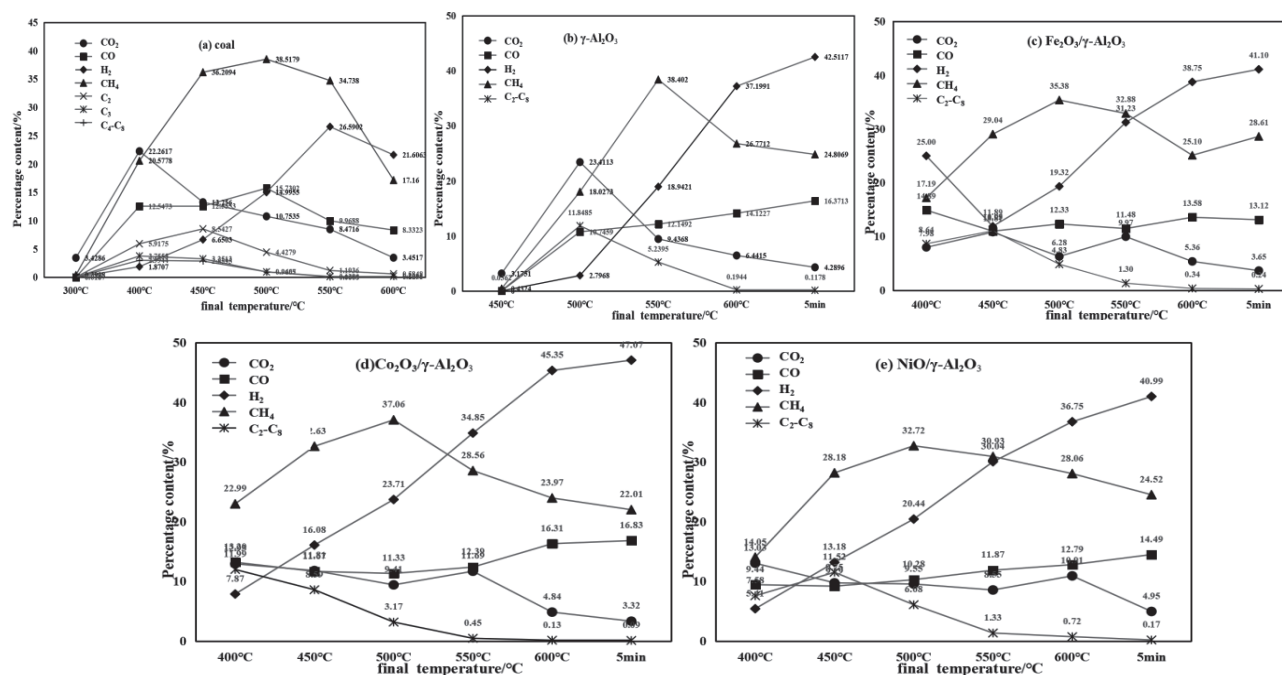


Fig. 3. The effect of subgroup metal oxide supported $\gamma-Al_2O_3$ catalyst on coal pyrolysis gas composition a) coal, b) $\gamma-Al_2O_3$, c) $Fe_2O_3/\gamma-Al_2O_3$, d) $Co_2O_3/\gamma-Al_2O_3$, e) $NiO/\gamma-Al_2O_3$.

600°C and the final temperature was 600°C and kept for 5min, the H_2 content reach the maximum, and the CO content reach the maximum when the final temperature was 600°C and kept for 5min. Coal pyrolysis can be roughly divided into three stages [18]. The first stage was from room temperature to 350°C, which was dry and degassing, mainly due to physical changes. The second stage was 350°C to 550°C, mainly depolymerization and decomposition, a large number of volatile gas and tar was also the process of coal bonding into coke. The third stage was 550°C to 1000°C, the secondary degassing was mainly condensation polymerization, the tar was less, the volatiles were mainly hydrocarbon gases, hydrogen and carbon oxides. The maximum total contents of CO, H_2 and CH_4 produced by pyrolysis of raw coal, $\gamma-Al_2O_3$, $Fe_2O_3/\gamma-Al_2O_3$ catalyst, $Co_2O_3/\gamma-Al_2O_3$ catalyst and $NiO/\gamma-Al_2O_3$ catalyst were 71.40%, 83.69%, 82.83%, 85.91% and 80.00%, respectively. The corresponding pyrolysis conditions were 550°C, 600°C for 5min, 600°C for 5min, 600°C for 5min, 600°C for 5min. According to the above analysis, $Co_2O_3/\gamma-Al_2O_3$ catalyst had a better effect on the catalytic pyrolysis of coal to produce hydrogen-rich fuel gas.

Effect of Group VIII Metal Oxide Supported $\gamma-Al_2O_3$ Catalyst on Coal Pyrolysis Products

Effect of Group VIII Metal Oxide Supported $\gamma-Al_2O_3$ Catalyst on Gas, Oil and Loss

Fig. 4 was the change of gas product and tar by putting 15 g coal sample and 3 g group VIII metal

oxide supported $\gamma-Al_2O_3$ catalyst into the pyrolysis furnace at the final temperature of 600°C and constant temperature of 5 min. It can be seen from Fig. 4 that the liquid and gas contents were increased by adding $CuO/\gamma-Al_2O_3$, $ZnO/\gamma-Al_2O_3$, $Mo_2O_3/\gamma-Al_2O_3$, $Cr_2O_3/\gamma-Al_2O_3$ and $Mn_2O_3/\gamma-Al_2O_3$ during coal pyrolysis, and $Cr_2O_3/\gamma-Al_2O_3$ resulted in the highest tar yield of 0.71 g, which was 121.88% higher than that of raw coal. The gas production was also the highest, at 1.73 g, which was 9.5% higher than that of raw coal. When coal and $Cr_2O_3/\gamma-Al_2O_3$ were pyrolyzed together, the contact between coal and active sites on $Cr_2O_3/\gamma-Al_2O_3$ surface resulted in the breaking of macromolecular chains in coal, which promoted the pyrolysis of coal and produced more pyrolytic products. The pyrolytic products came into contact with active Cr_2O_3 inside $Cr_2O_3/\gamma-Al_2O_3$, and further caused the breaking of macromolecules to produce small molecules, which were easy to vaporize and volatilize at higher temperature, therefore, $Cr_2O_3/\gamma-Al_2O_3$ made the total amount of tar and gas produced in the mixed pyrolysis process the highest, and the catalytic effect was the best.

Effect of Group VIII Metal Oxide Supported $\gamma-Al_2O_3$ Catalyst on Gas Components

Fig. 5(a-e) respectively represented adding $CuO/\gamma-Al_2O_3$ catalyst, $ZnO/\gamma-Al_2O_3$ catalyst, $Mo_2O_3/\gamma-Al_2O_3$ catalyst, $Cr_2O_3/\gamma-Al_2O_3$ catalyst and $Mn_2O_3/\gamma-Al_2O_3$ catalyst, and the gas composition changed with the pyrolysis temperature. In Fig. 5, it can be seen that the change trend of gas with pyrolysis temperature was basically the same after adding different catalysts, and

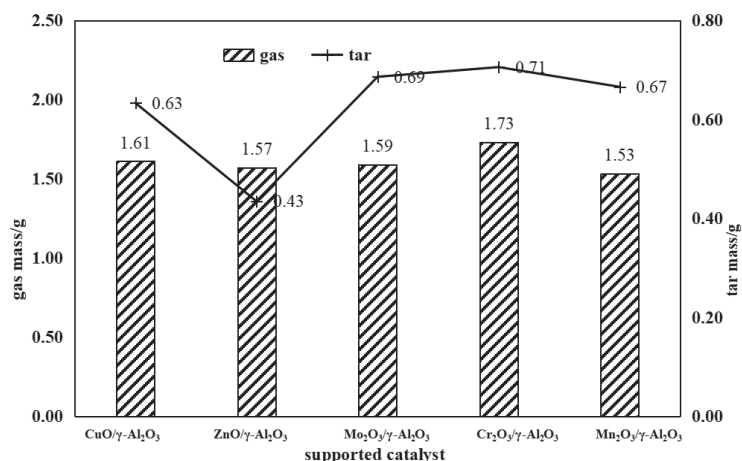


Fig. 4. Effect of group VIII metal oxide supported γ -Al₂O₃ catalyst on gas and tar.

the content of CH₄ reached the maximum when the pyrolysis temperature reached 500°C to 550°C. When the pyrolysis temperature reached 600°C and the final temperature reached 600°C for 5 min, the content of H₂ was the maximum. And the content of CO reached the maximum at the final temperature of 600°C for 5 min. The maximum total contents of CO, H₂ and CH₄ produced by pyrolysis of CuO/γ-Al₂O₃ catalyst, ZnO/γ-Al₂O₃ catalyst, Mo₂O₃/γ-Al₂O₃ catalyst, Cr₂O₃/γ-Al₂O₃ catalyst and Mn₂O₃/γ-Al₂O₃ catalyst were 79.62%, 80.66%, 79.96%, 87.31% and 74.95%, respectively. The corresponding pyrolysis conditions were 600°C for 5 min, 600°C for 5 min, 600°C for 5 min, 600°C for 5 min and 550°C. According to the above analysis, Cr₂O₃/γ-Al₂O₃ catalyst had a better effect on the

catalytic pyrolysis of coal to produce hydrogen-rich fuel gas.

Effect of Different Loading Cr₂O₃/γ-Al₂O₃ Catalyst on Coal Pyrolysis Products

Effect of Different Loading Cr₂O₃/γ-Al₂O₃ Catalyst on Gas and Tar

Fig. 6 shows the change of gas product and tar by putting 15 g coal sample and 3 g Cr₂O₃/γ-Al₂O₃ catalyst with loading of 1%, 5% and 11% into the pyrolysis furnace at the final temperature of 600°C and constant temperature of 5 min. As can be seen from Fig. 6, the liquid and gas contents increased with the addition of

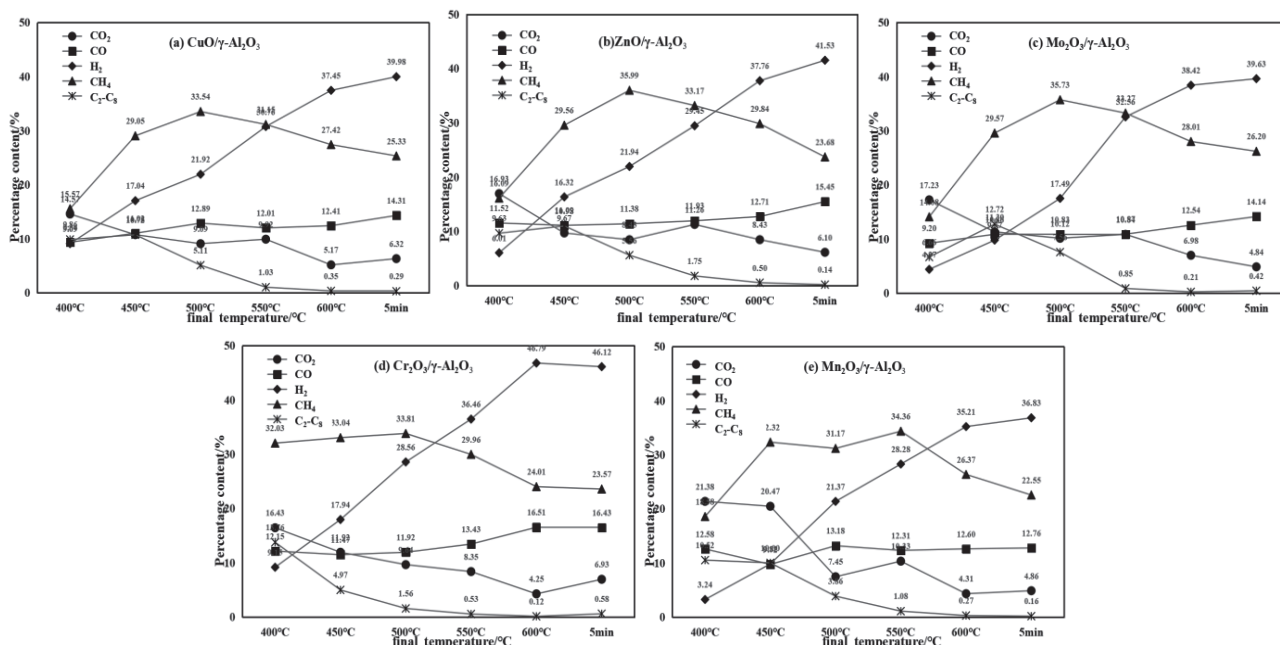


Fig. 5. Effect of group VIII metal oxide supported γ -Al₂O₃ catalyst on gas components a) CuO/γ-Al₂O₃, b) ZnO/γ-Al₂O₃, c) Mo₂O₃/γ-Al₂O₃, d) Cr₂O₃/γ-Al₂O₃, e) Mn₂O₃/γ-Al₂O₃.

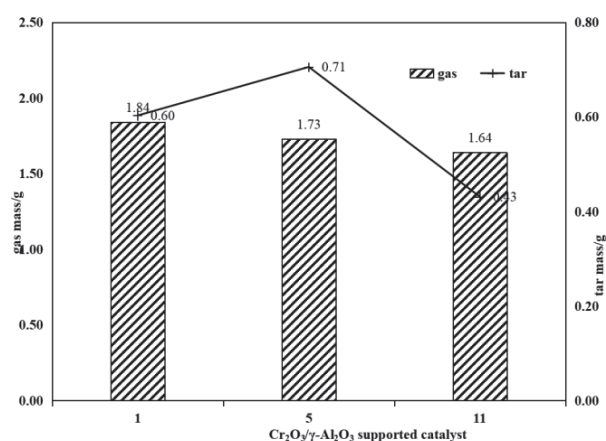


Fig. 6. Effect of $\text{Cr}_2\text{O}_3/\gamma\text{-Al}_2\text{O}_3$ catalysts with different loading loads on gas and tar.

$\text{Cr}_2\text{O}_3/\gamma\text{-Al}_2\text{O}_3$ catalysts with different loading during coal pyrolysis, but the liquid and gas contents decreased with the increase of loading. A large amount of active components were produced in $\gamma\text{-Al}_2\text{O}_3$ carrier after calcination, which greatly improved the activity of the catalyst. However, the active components can easily block the internal channels of the carrier, thus reducing the specific surface area and pore diameter, and thus reducing the number of tar molecules entering the catalyst, this further reduced tar production and gas production. So when the load was 1%, the liquid and gas production was the largest.

Effect of Different Loading $\text{Cr}_2\text{O}_3/\gamma\text{-Al}_2\text{O}_3$ Catalyst on Gas Components

Fig. 7 shows that 15 g coal sample and 3 g $\text{Cr}_2\text{O}_3/\gamma\text{-Al}_2\text{O}_3$ catalyst with 1%, 5% and 11% loading was mixed evenly and pyrolyzed in a pyrolyzer, and the gas composition changed with the pyrolysis temperature. In Fig. 7, it can be seen that the change trend of gas with pyrolysis temperature was basically the same. The content of CH_4 reached the maximum

when the pyrolysis temperature reached 500°C. The content of H_2 reached the maximum when the pyrolysis temperature reached 600°C and 600°C for 5 min. The content of CO reached the maximum when the final temperature was 600°C and constant temperature was 5 min. The highest total contents of CO, H_2 and CH_4 were 88.48%, 87.31% and 80.42% respectively when $\text{Cr}_2\text{O}_3/\gamma\text{-Al}_2\text{O}_3$ catalysts with 1%, 5% and 11% loading were pyrolyzed. The corresponding pyrolytic conditions were all 600°C. Based on the above analysis, the effect of $\text{Cr}_2\text{O}_3/\gamma\text{-Al}_2\text{O}_3$ catalyst on the preparation of hydrogen-rich fuel gas was better than that of $\text{Cr}_2\text{O}_3/\gamma\text{-Al}_2\text{O}_3$ catalyst with 1% loading. According to the above analysis, when the catalyst load was 1%, $\text{Cr}_2\text{O}_3/\gamma\text{-Al}_2\text{O}_3$ catalyst had a better effect on the catalytic pyrolysis of coal to produce hydrogen-rich fuel gas.

Characterization

BET

Table 3 showed the specific surface area of different $\gamma\text{-Al}_2\text{O}_3$ catalysts. In the process of coal pyrolysis, oil vapor molecules from coal entered the catalyst and contacted with the active site to produce small molecular substances, the specific surface area and pore size of catalysts played an important role in catalytic cracking of oil vapor molecules. It can be seen from Table 3 that the specific surface area of $\gamma\text{-Al}_2\text{O}_3$ is 271.64 m^2/g , and the specific surface areas of $\text{Fe}_2\text{O}_3/\gamma\text{-Al}_2\text{O}_3$, $\text{Co}_2\text{O}_3/\gamma\text{-Al}_2\text{O}_3$, $\text{Ni}_2\text{O}_3/\gamma\text{-Al}_2\text{O}_3$, $\text{CuO}/\gamma\text{-Al}_2\text{O}_3$, $\text{ZnO}/\gamma\text{-Al}_2\text{O}_3$, $\text{Mo}_2\text{O}_3/\gamma\text{-Al}_2\text{O}_3$, $\text{Cr}_2\text{O}_3/\gamma\text{-Al}_2\text{O}_3$ and $\text{Mn}_2\text{O}_3/\gamma\text{-Al}_2\text{O}_3$ decreased after loading, the reason was that the catalyst after being loaded was calcined to form oxide, which clogged the pore channels of the support and lead to a small specific surface area. However, $\gamma\text{-Al}_2\text{O}_3$ and $\text{Cr}_2\text{O}_3/\gamma\text{-Al}_2\text{O}_3$ had better catalytic cracking effect on coal pyrolysis, which was due to their large specific surface area, better adsorption of oil and gas molecules and contacted with active sites.

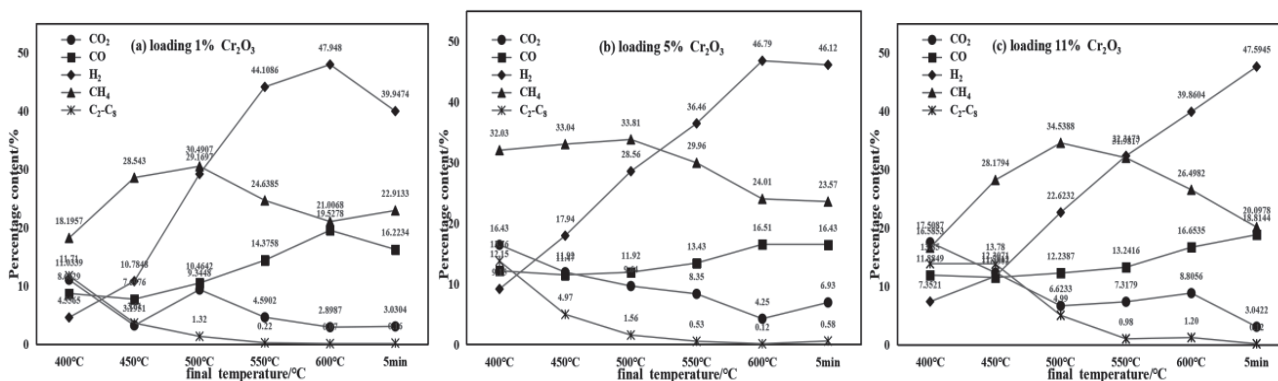


Fig. 7. Effect of different loading $\text{Cr}_2\text{O}_3/\gamma\text{-Al}_2\text{O}_3$ on gas components a) loading 1% $\text{Cr}_2\text{O}_3/\gamma\text{-Al}_2\text{O}_3$, b) loading 5% $\text{Cr}_2\text{O}_3/\gamma\text{-Al}_2\text{O}_3$, c) loading 11% $\text{Cr}_2\text{O}_3/\gamma\text{-Al}_2\text{O}_3$.

Table 3. specific surface area of γ -Al₂O₃ catalyst (m²/g).

Catalyst	Specific surface area	Catalyst	Specific surface area
γ -Al ₂ O ₃	271.64	CuO/ γ -Al ₂ O ₃	200.34
Fe ₂ O ₃ / γ -Al ₂ O ₃	251.88	ZnO/ γ -Al ₂ O ₃	203.12
Co ₂ O ₃ / γ -Al ₂ O ₃	249.67	Mo ₂ O ₃ / γ -Al ₂ O ₃	247.99
Ni ₂ O ₃ / γ -Al ₂ O ₃	250.20	Cr ₂ O ₃ / γ -Al ₂ O ₃	258.43
		Mn ₂ O ₃ / γ -Al ₂ O ₃	245.77

XRD

Fig. 8 showed the XRD patterns of Fe₂O₃/ γ -Al₂O₃, Co₂O₃/ γ -Al₂O₃, Ni₂O₃/ γ -Al₂O₃, CuO/ γ -Al₂O₃, ZnO/ γ -Al₂O₃, Mo₂O₃/ γ -Al₂O₃, Cr₂O₃/ γ -Al₂O₃ and Mn₂O₃/ γ -Al₂O₃. As can be seen from Fig. 8, the impregnated γ -Al₂O₃ formed corresponding metal oxides on the catalyst after roasting in a muffle furnace. In Fig. 8(1), the 2θ angles of 32.78°, 36.54°, 37.51°, 43.17°, 45.79°, 66.76° and 67.31° were the characteristic peaks of γ -Al₂O₃ [19]. In Fig. 8(2), the 2θ angles 36.04°, 41.92°, 60.69° and 61.25° were the characteristic peaks of FeO, and the 2θ angles 14.73°, 24.71°, 31.13°, 32.98°,

35.68°, 38.10°, 47.30°, 54.90°, 67.10° and 70.18° were the characteristic peaks of Fe₂O₃ [20]. In Fig. 8(3), 2θ angles 34.15°, 36.49°, 42.39°, 57.30° and 61.52° were characteristic peaks of CoO; 2θ angles 31.27°, 36.85°, 44.80°, 59.35° and 65.23° were characteristic peaks of Co₃O₄; 2θ angles 27.77°, 31.14°, 38.61°, 51.28°, 56.40°, 58.76° and 67.31° were characteristic peaks of Co₂O₃ [21]. In Fig. 8(4), 2θ angles 37.25° and 43.29° were the characteristic peaks of NiO, 2θ angles 31.94°, 39.13°, 44.83°, 51.59°, 56.78°, 66.71° and 87.89° were the characteristic peaks of Ni₂O₃ [22]. In Fig. 8(5), 2θ angles 32.50°, 35.50°, 38.47°, 48.59°, 61.34° and 67.85° were characteristic peaks of CuO, and 2θ angles 37.01°,

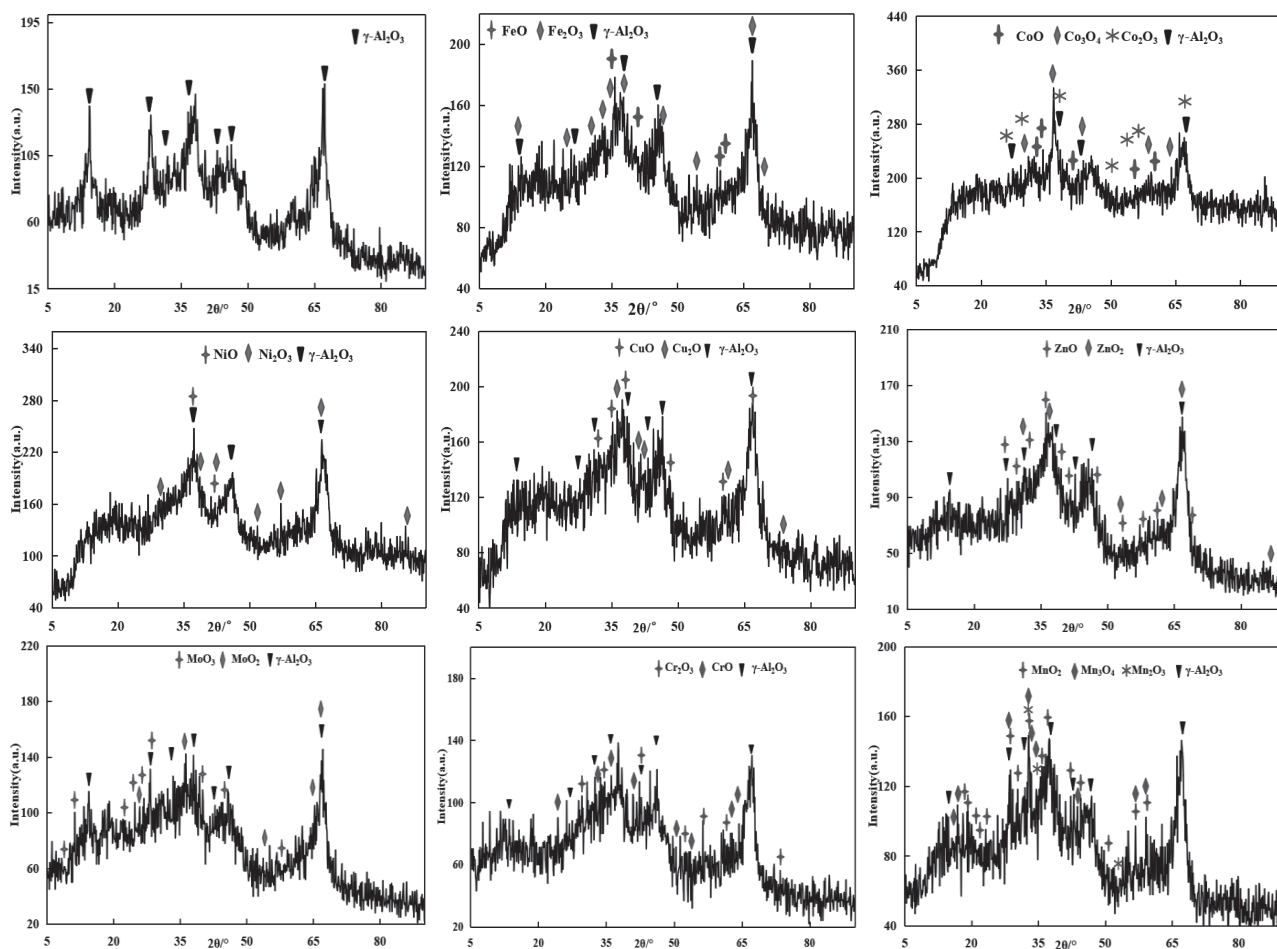


Fig. 8. XRD of γ -Al₂O₃ catalyst (1) γ -Al₂O₃, (2) Fe₂O₃/ γ -Al₂O₃, (3) Co₂O₃/ γ -Al₂O₃, (4) NiO/ γ -Al₂O₃, (5) CuO/ γ -Al₂O₃, (6) ZnO/ γ -Al₂O₃, (7) Mo₂O₃/ γ -Al₂O₃, (8) Cr₂O₃/ γ -Al₂O₃, (9) NiO/ γ -Al₂O₃.

Table 4. Metal element determination results of supported $\gamma-Al_2O_3$ catalyst (%).

Catalyst	Elements	Theoretical value	Determination of value	Load factor
$Fe_2O_3/\gamma-Al_2O_3$	Fe	3.50	3.01	86.00
$Co_2O_3/\gamma-Al_2O_3$	Co	3.55	3.05	85.92
$Ni_2O_3/\gamma-Al_2O_3$	Ni	3.58	3.08	86.03
$CuO/\gamma-Al_2O_3$	Cu	4.00	3.40	85.00
$ZnO/\gamma-Al_2O_3$	Zn	4.01	3.47	86.53
$Mo_2O_3/\gamma-Al_2O_3$	Mo	6.67	5.72	85.76
$Cr_2O_3/\gamma-Al_2O_3$	Cr	3.42	3.00	87.72
$Mn_2O_3/\gamma-Al_2O_3$	Mn	3.48	3.01	86.49

40.64°, 42.61°, 62.44° and 74.40° were characteristic peaks of Cu_2O [23]. In figure 8(6), 2 θ angles 26.68°, 30.92°, 33.67°, 36.50°, 39.13°, 41.99°, 47.57°, 54.58°, 58.76°, 62.73° and 69.58° were characteristic peaks of ZnO, while 2 θ angles 31.90°, 36.99°, 53.21°, 63.30°, 66.60° and 87.20° were characteristic peaks of ZnO [24]. In figure 8(7), 2 θ angles of 9.69°, 12.84°, 23.01°, 25.80°, 39.13°, 27.41°, 29.36°, 39.19°, 45.90° and 58.82° were characteristic peaks of MoO_3 , and 2 θ angles of 26.03°, 36.52°, 53.79°, 65.70° and 66.66° were characteristic peaks of MoO_2 [25]. In Fig. 8(8), 2 θ angles 34.60°, 30.27°, 23.01°, 43.25°, 57.17° and 62.82° were characteristic peaks of CrO, and 2 θ angles 24.49°, 33.60°, 36.20°, 41.48°, 50.22° and 54.85° were characteristic peaks of Cr_2O_3 [26]. In Fig. 8(9), 2 θ angles 18.11°, 19.76°, 21.81°, 22.84°, 23.97°, 28.84°, 31.58°, 33.28°, 36.96°, 37.52°, 42.61°, 45.09°, 49.86°, 56.04° and 60.27° were characteristic peaks of Mn_2O_3 , 2 θ angles 32.92°, 35.60° and 53.21° were characteristic peaks of Mn_2O_3 , and 2 θ angles 17.55°, 18.02°, 28.97°, 32.41°, 34.06°, 35.31°, 44.37°, 56.78°, 60.02° and 62.35° were characteristic peaks of Mn_3O_4 [27]. Diffraction peak strength was large, the popularity was sharp, the formation of oxide dispersion was good, increased the catalytic activity of the catalyst. Combined with the results of specific surface area, although the specific surface area of $Cr_2O_3/\gamma-Al_2O_3$ was smaller than the surface of $\gamma-Al_2O_3$, but in the $Cr_2O_3/\gamma-Al_2O_3$ catalyst formed active Cr_2O_3 , improved the catalytic activity, so $Cr_2O_3/\gamma-Al_2O_3$ on coal pyrolysis catalytic cracking effect was the best.

Table 5. Cr element determination results of $Cr_2O_3/\gamma-Al_2O_3$ catalyst (%)

Load capacity	Elements	Theoretical value	Determination of value
1	0.68	0.66	97.06
5	3.42	3.00	87.72
8	5.47	4.43	81.04

Determination of Metal Element Loading Amount of Catalyst by ICP-MS

Table 4 showed the results of metal element loading of $\gamma-Al_2O_3$ catalysts with different metal supports. It can be seen from Table 4, ICP-MS [28] determined metal element, and the actual content and the theoretical content of metal elements had certain difference, that the metal in the process of load had a certain loss, but each metal elements of effective negative rate were over 85%, among them $Cr_2O_3/\gamma-Al_2O_3$ catalyst metal elements Cr payload rate was as high as 87.72%, which proved more metal oxide was formed on the catalyst carrier, and ensured the activity of catalyst.

Table 5 showed the results of determination of Cr element in $Cr_2O_3/\gamma-Al_2O_3$ catalyst by ICP-MS. It can be seen from table 5 that with the increase of load, the payload rate decreased. When the load was 1%, the effective load was the highest, and the highest value was 97.06%. The reason was that the pore size of $\gamma-Al_2O_3$ was certain, the loading capacity was small, the solution concentration was low, the metal element Cr was easy to be adsorbed. When the loading capacity increased, the solution concentration was higher, and the adsorption of metal element Cr was easy to reach saturation, so the loading rate became smaller.

Conclusions

The liquid yield and gas yield of raw coal pyrolysis were 0.32 g and 1.58 g, respectively. The maximum total contents of CO, H₂ and CH₄ produced by raw coal pyrolysis were 71.40%, respectively.

Different oxides supported $\gamma-Al_2O_3$ catalysts were added to the coal samples for mixed pyrolysis. $Fe_2O_3/\gamma-Al_2O_3$ catalysts made the highest of the tar yield, it was 0.71g, and which was 134.38% higher than that of raw coal pyrolysis. $Cr_2O_3/\gamma-Al_2O_3$ catalyst also resulted in the highest gas yield, it was 1.73g, and which was 9.5% higher than raw coal. The highest contents of CO, H₂ and CH₄ were produced during the pyrolysis of $Cr_2O_3/\gamma-Al_2O_3$ catalyst, which was 87.31%, and the

pyrolysis condition was 600°C for 5 min. Cr₂O₃/γ-Al₂O₃ catalyst prepared with 1% Cr₂O₃ support had a good catalytic effect on coal mixed pyrolysis.

The catalyst after being loaded was calcined to form oxide, which clogged the pore channels of the support and lead to a small specific surface area. So the specific surface area of the catalyst had a great influence on the pyrolysis products of the mixture of catalyst and coal, and the larger the specific surface area was, the better the pyrolytic cracking effect was. The specific surface area of γ-Al₂O₃ was 271.64, the specific surface area of Cr₂O₃/γ-Al₂O₃ and γ-Al₂O₃ was similar, which was led to better adsorption of oil and gas molecules and contacted with active sites. The catalytic cracking effect of Cr₂O₃/γ-Al₂O₃ was more obvious than that of γ-Al₂O₃, so the catalytic activity of Cr₂O₃ was higher. By ICP-MS detection of load metal element content, it found that the load rate was relatively high, and the smaller the load the higher the load rate.

Acknowledgments

Financial support of this research was provided by Key Laboratory of Coal Resources Exploration and Comprehensive Utilization, Ministry of Land and Resources (Program No.KF2020-10) in P.R. China. Project 51704230 supported by National Natural Science Foundation of China.

Conflict of Interest

The authors declare no conflict of interest.

Reference

- MENG D.X., YUE C.Y., WANG T., CHEN X.L. Evolution of carbon structure and functional group during Shenmu lump coal pyrolysis. *Fuel*, **287**, 1, **2021**.
- GUO X., TANG Y.G., WANG Y.F., EBLE C.F., FINKELMAN R.B., HUAN B.B., PAN X. Potential utilization of coal gasification residues from entrained-flow gasification plants based on rare earth geochemical characteristics. *Journal of Cleaner Production*, **280**, 1, **2021**.
- GAO L.F., LIU X.C., BAI J., et al. Structure and flow properties of coal ash slag using ring statistics and molecular dynamics simulation: Role of CaO/Na₂O in SiO₂-Al₂O₃-CaO-Na₂O [J]. *Chemical Engineering Science*, **231**, 1, **2021**.
- GAO H.S., ZONG Z.M., LI J.H., KONG L.X., BAI Z.Q., LI W. Characterization of Oxygen-Containing Aromatics in a Low-Temperature Coal Tar. *Energy & Fuels*, **31** (1), 283, **2021**.
- YUAN X., QING M.L., MENG L.Q., ZHAO H.B. One-Step Synthesis of Nanostructured Cu-Mn/TiO₂ via Flame Spray Pyrolysis: Application to Catalytic Combustion of CO and CH₄. *Energy & Fuels*, **34** (11), 14447, **2020**.
- HAN D.H., HU Y.Q., WANG J.S., YAO R., SHAO J.X. Study and Analysis of Influence Factors of Coal Pyrolysis. *Coal Technology*, **30** (7), 164, **2011**.
- WANG J.H., CHANG L.P., XIE K.C. Study on the pyrolysis and kinetics of coal of wewtern China. *Coal Conversion*, **32** (3), 1, **2009**.
- ZHANG Q.L., LI F.Y., HUI X.R. LUO M., ZHOU J. Evolution Characteristics of Gas Products in Pyrolysis Process of Low Metamorphic Coal [J]. *Coal Conversion*, **42** (4), 32, **2019**.
- LIU Q.F., CUI X.N., XU Z.J., ZHENG Q.M., WU Y.K. Main gases and kinetics of coal pyrolysis [J]. *Coal Geology & Exploration*, **44** (6), 27, **2016**.
- WANG K.F., QIAN J., SUN F., TIAN Z.Q., GAO J.H., ZHAO G.B. In-situ catalytic conversion of coal pyrolysis gas to nanoporous carbon rods and superior sodium ion storage performance. *Fuel*, **281**, 1, **2020**.
- CHEN Q.L., FANG M.X., CEN J.M., ZHAO Y.F., WANG Q.H., WANG Y.W. Electrostatic precipitation under coal pyrolysis gas at high temperatures. *Powder Technology*, **362**, 1, **2020**.
- ZHENG C.H., LIU X.T., XU X., YAN P., CHANG Q.Y., WANG Y., GAO X. Experimental study on electrostatic removal of high-carbon particle in high temperature coal pyrolysis gas. *Proceedings of the Combustion Institute*, **37** (3), 2959, **2019**.
- LI Z., ZHAO X.C., MIAO B.B., JIANG Y.R., ZHAO Y.J. Preparation of Supported Fe₂O₃/γ-Al₂O₃ Catalyst and Its Performance in Microwave Pyrolysis of Coal. *Journal of Materials Science and Engineering*, **32** (6), 826, **2014**.
- YAN H., GONG M.G., WANG J.Y., WANG C.P. Anti-Carbon Deposition Performance of Ca-Mg Catalyst in Coal Tar Catalytic Cracking Process. *Acta Petrolei Sinica(Petroleum Processing Section)*, **36** (04), 832, **2020**.
- ZHANG Y.M., ZOU D., ZHAO Y., ZHONG M., MA F.Y. Effect of bimetallic catalysts on cracking behavior of coal tar model compounds. *CIESC Journal*, **68** (10), 3805, **2017**.
- MEROUFEL B., ZENASNI M.A., GEORGE B. Valorisation and Modification of Saharan Clay for Removal of Cu(II), Ni(II), Co(II) and Cd(II) from Aqueous Solutions. *Polish Journal of Environmental Studies*, **29** (2), 1287, **2020**.
- HU N.F., CUI H.T., QIU Z.G. ZHAO L.F., MENG Xi.X., ZHAO Z.Q., AO G.Y. Effect of phosphorus loadings on the performance of Co-Mo/γ-Al₂O₃ in hydrodesulfurization of coal tar. *Journal of Fuel Chemistry and Technology*, **44** (6), 745, **2016**.
- ZHANG P.W., WANG B., TIAN W.D., YANG S.J., XIAO Y.H. Influences of mixing methods on CaO/char steam gasification. *Journal of China Coal Society*, **41** (8), 2097, **2016**.
- ZHANG L., CHRN J.H., ZHANG L., SHA, X.L., LI Y.H., Fan M. Preparing Mn-CoO-Supported Pyrolysis Coke Catalyst with Plasma and its Application in the SCO Denitration Process. *Polish Journal of Environmental Studies*, **28** (5), 3323, **2019**.
- LIU W.S., HUANG B.F., LIU L.P., ZHAO H.W., ZHAO S.M., PAN C.L., LIU H.W. Preparation and characterization of supported γ-Fe₂O₃ coconut shell activated carbon catalyst. *Carbon Techniques*, **38** (06), 49, **2019**.
- TANG W.D., YANG S.T., YANG H., XUE X.X. Effect of Co₂O₃ on Oxidation Induration and Reduction Swelling of Chromium-Bearing Vanadium Titanomagnetite Pellets with Simulated Coke Oven Gas. *Metals*, **9** (01), 1, **2018**.

22. YU H.F., CHEN C.L., WANG Y.J., LUO M.F. Ozone Decomposition over NiO/Mn₃O₄ Monolithic Catalysts. Chinese Journal of Applied Chemistry, **36** (06), 698, **2019**.
23. LIN M., NA W., YE H.C., HUO H.H., GAO W.G. Effect of different promoters on CuO-ZnO/SBA-15 catalytic performance of CO₂ hydrogenation to methanol. Journal of Fuel Chemistry and Technology, **47** (10), 1214, **2019**.
24. HE Z.M., XIA Y.M., TANG B., JIANG X.F., HUANG Z.Y. Preparation and Photocatalytic Property of ZnO/Cu₂O Heterostructured Nanorod Arrays. Chinese Journal of Luminescence, **38** (07), 936, **2017**.
25. HUANG P., LIU M., CHANG Q.L. MoO₃/Al-SBA-15 modified catalyst and its application in coal tar hydrocracking. Journal of Fuel Chemistry and Technology, **48** (09), 1079, **2020**.
26. WU T.X., YANG Y.W., CAI Q., SUN Y.M., YU H.B. Catalytic performance of CrOx/Al₂O₃ for dehydrogenation of propane. Natural Gas Chemical Industry, **41** (03), 16, **2016**.
27. WANG Z.J., SOHN I. Immobilizing chromium in stainless steel slags with MnO addition. Journal of the American Ceramic Society, **104** (2), 697, **2021**.
28. YE J.M., WU B.L., WANG H., YUAN L.F., LUO C. Determination of fourteen elements residues of catalysts in plastics [J]. Chinese Journal of Analysis Laboratory, **31** (09), 54, **2012**.

